Supplementary Materials

Molecular Biology of the Cell

Moore *et al*.

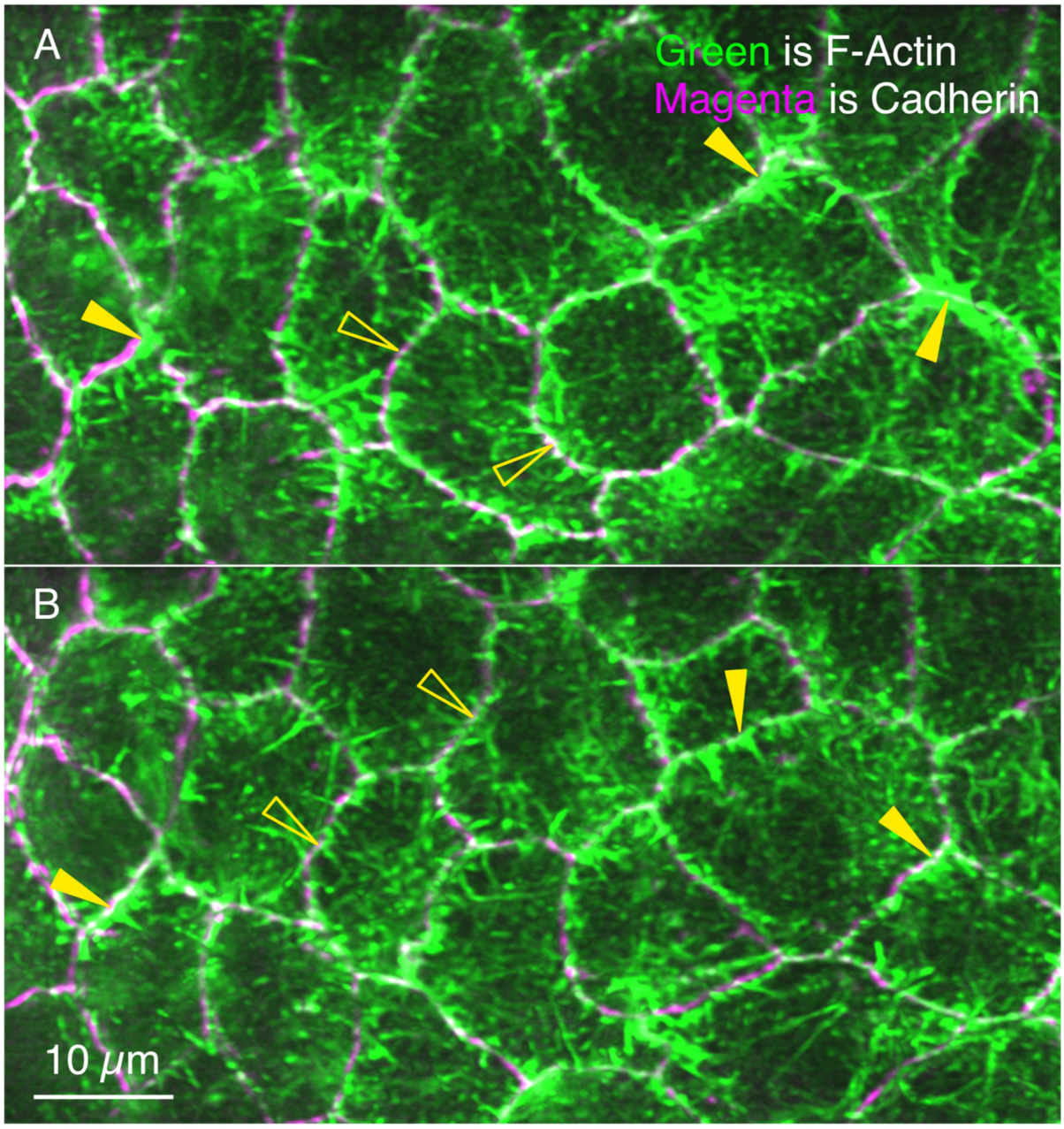

Supplemental Figure 1. Cell edges are marked by a profusion of actin-rich lamellipodia and filapodia shown superimposed on cell junctions marked with cadherin. Apical views of amnioserosa cells from a LLSM data set of an embryo labeled with GFP-MoeABD and *d*ECadherin-mTomato knockIn showing the profusion of lamellipodia and filopodia that appear to emanate from cell junctions. Images are projected from a thin slice of volume taken near the apical surface of the cell. Arrowheads point to lamellipodia; hollow arrowheads point to junctions from which filopodia protrude and are referenced in the main

text. Frames are from Supplemental Movie 3, which dynamically shows the relationship between cadherin rich junctions and the profusion of actin projections from those junctions.

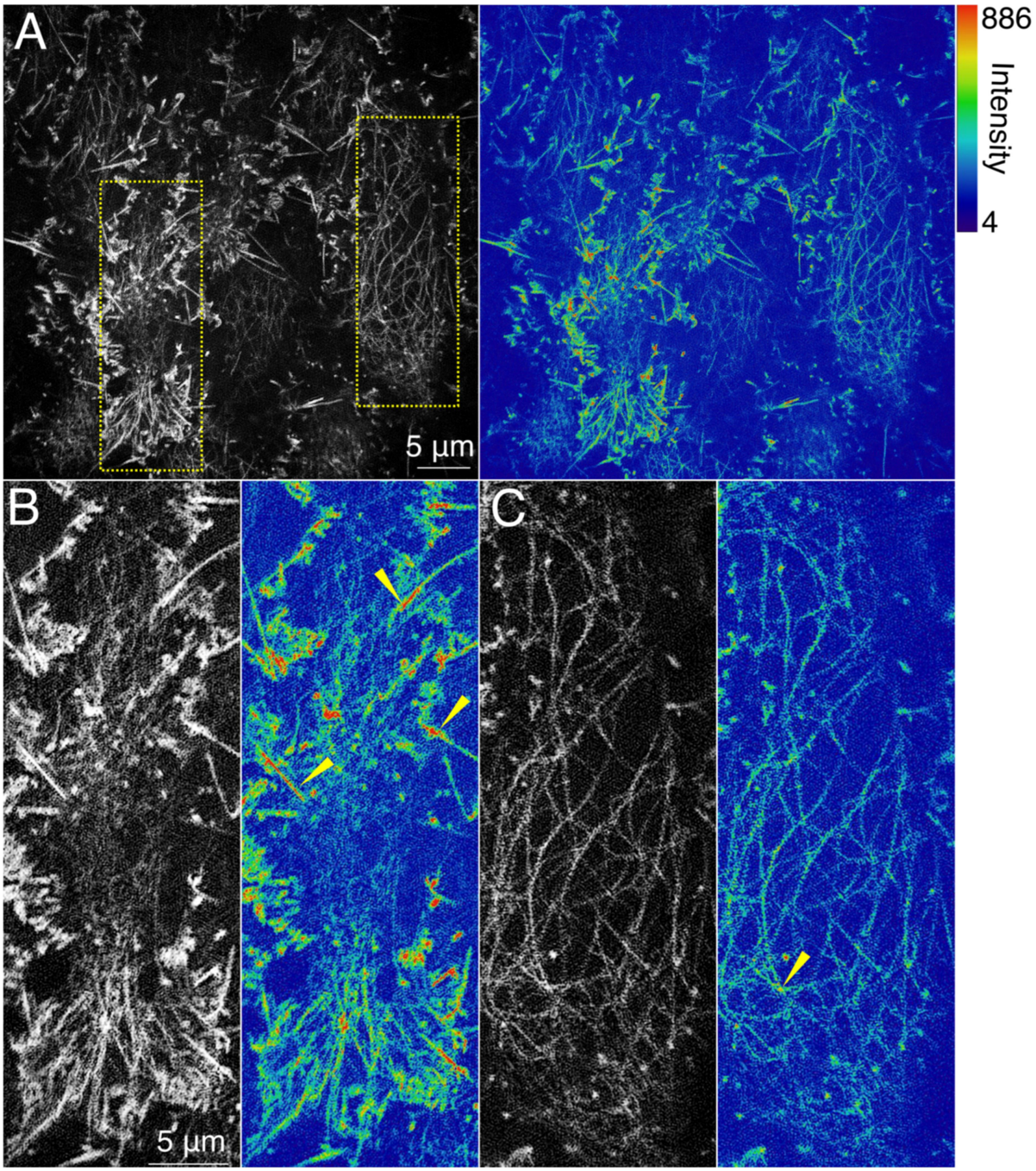

Supplemental Figure 2. Heat maps of actin intensity along filaments are consistent with uniform labeling of a single actin filament. The fluorescent intensity of medioapical array filaments is uniform and is dimmer than bundled filaments present in filopodia. F-actin is labeled with Lifeact-mEGFP. Arrowheads indicate regions of higher fluorescent intensity due

to multiple F-actin filaments either due to (B) Bundling of filopodia or (C) Crossing of multiple filaments within the medioapical array. Still images are from Supplemental Movie 2.

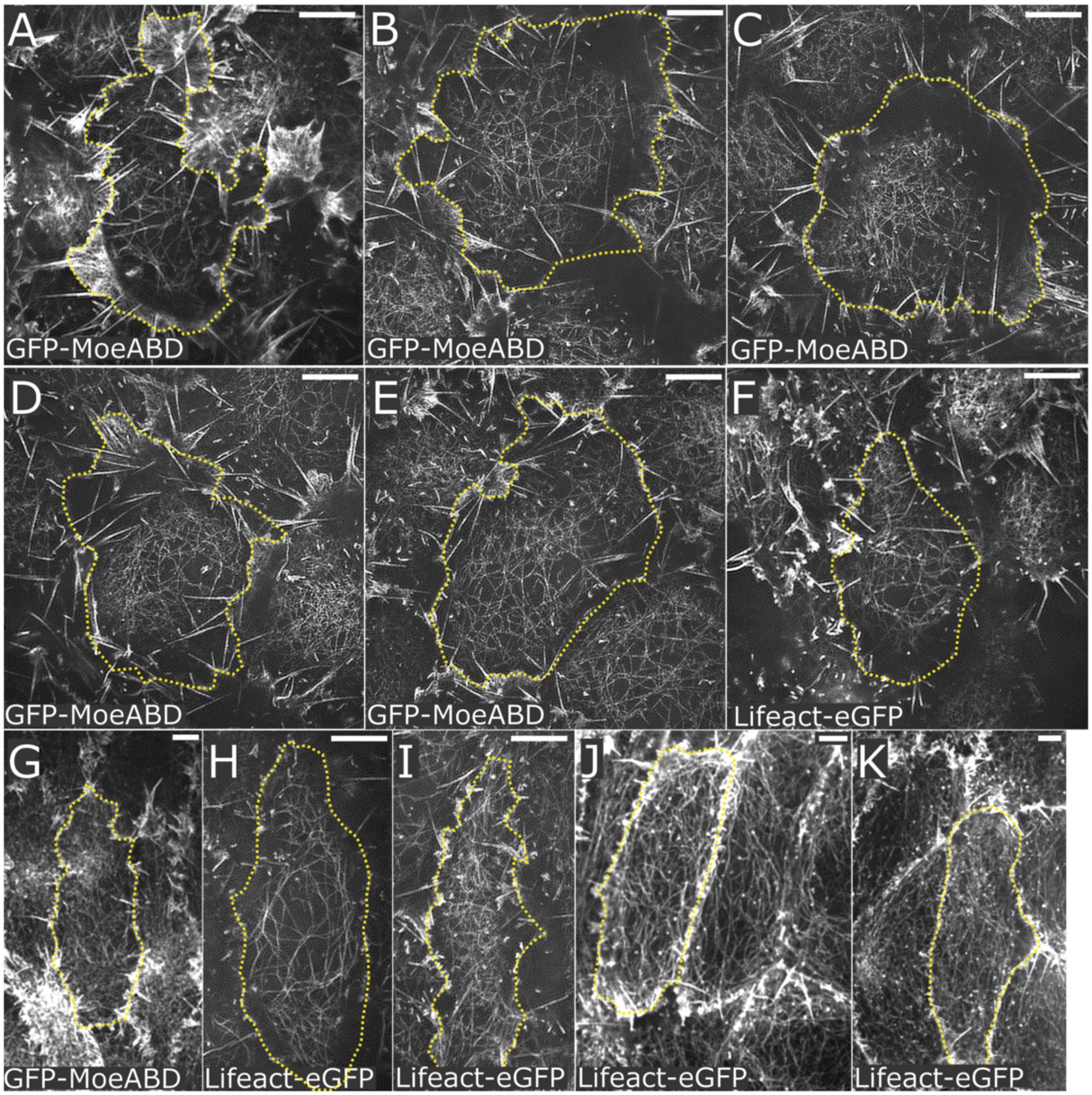

Supplemental Figure 3. Distribution of filament lengths are overlapping between GFP-MoeABD and Lifeact-mEGFP labeled isotropic and anisotropic cells. Panels A-F show the six isotropic cells from which we traced actin filaments and analyzed their alignment. Panels G-K show the five anisotropic cells from which we traced actin filaments and analyzed their alignment. We were able to find cells in both categories with different fluorescent actin markers, suggesting that cell shape and ability to trace filaments is not an artefact of the

labeling. The scale bars in all panels is 5um. The dashed yellow lines show the cell boundaries approximated by lamellipodial and filopodia protrusions. Panels G, J and K were taken on a new W-1 Yokogawa confocalling system which does not match the resolution provided by GI-SIM. Dynamics are also shown in Supplemental Movies 1, 2, 6 and 7.

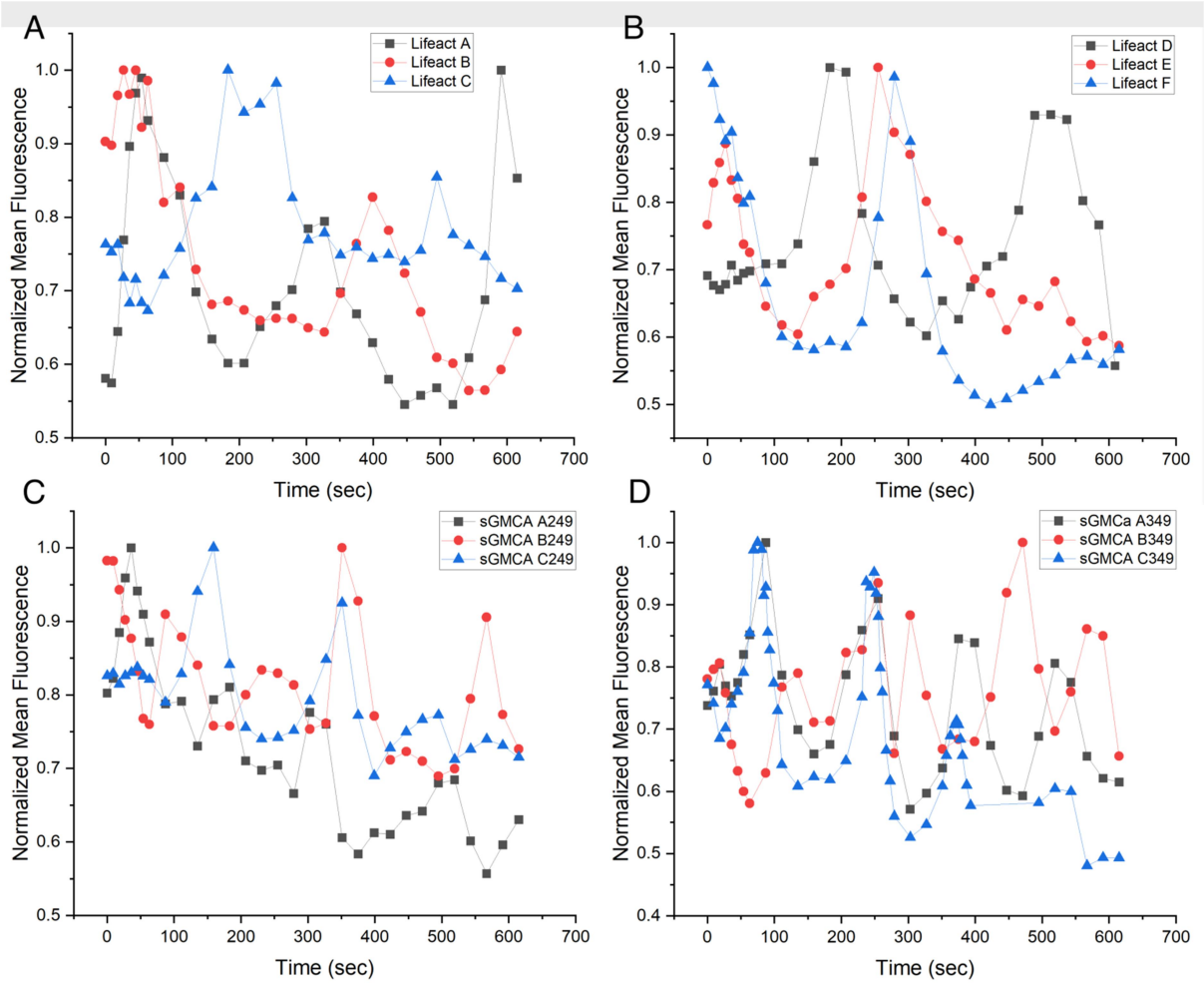

Supplemental Figure 4. Mean fluorescent intensity of medioapical arrays during amnioserosa cell oscillations. Intensity variation due to F-actin is substantial (~ 2 fold) with time, but the same type of changes are seen between actin markers (Lifeact-mEGFP in A and B, GFP-MoeABD in C and D). The mean fluorescence intensity for each of three cells are plotted in each graph to simplify following the cells analyzed.

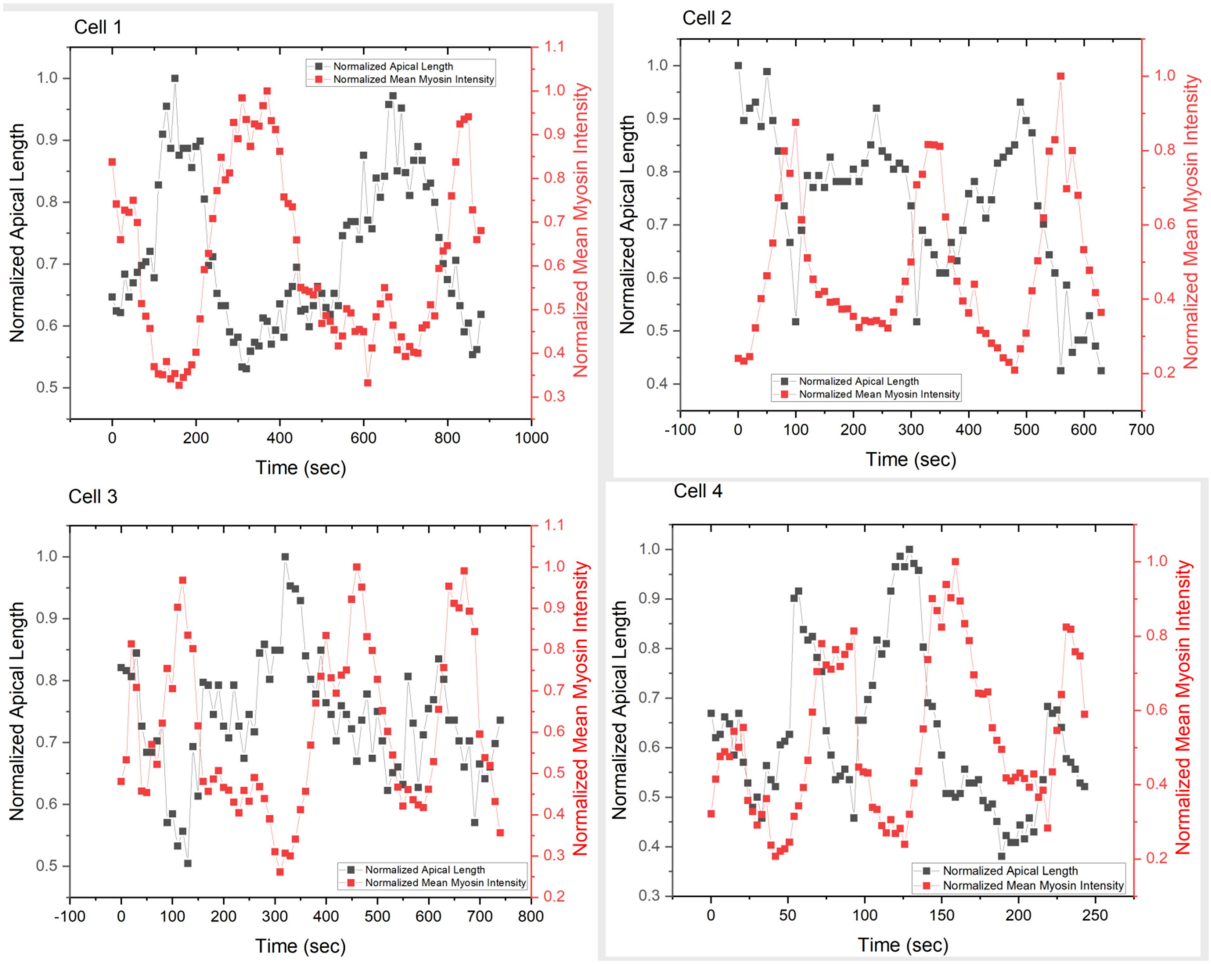

Supplemental Figure 5. Plots of normalized apical pathlength and normalized mean myosin accumulation along that pathlength demonstrate (anti-) correlation between myosin accumulation and cell bulging (see Materials and Methods). Four cells and a total of 12 bulges are shown. Dynamics of actin and myosin recruitment to the the membrane is shown in Supplemental Movie 10.

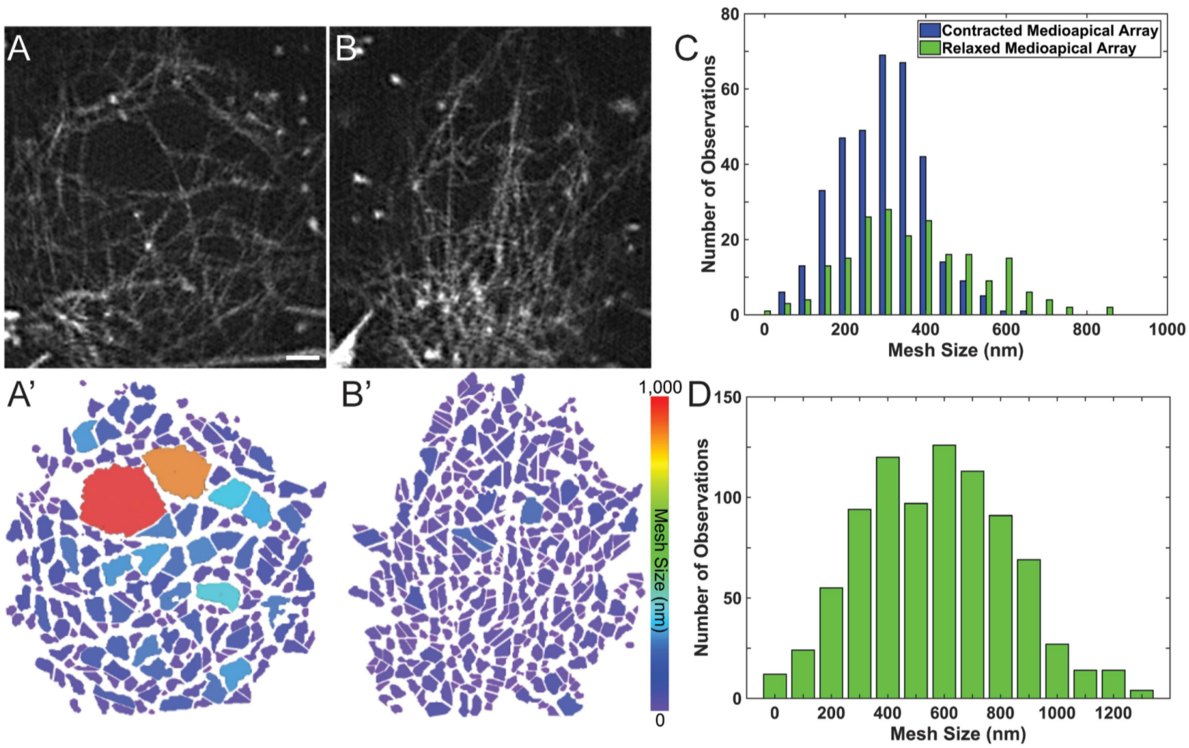

Supplemental Figure 6. Large mesh sizes characterize relaxed medioapical arrays. (A-B) A medioapical array labeled with GFP-MoeABD in the relaxed and condensed state. (A'-B') The medioapical array from (A-B) segmented and color coded to demonstrate the mesh size between F-actin filaments. (C) A histogram of the mesh sizes from (A'-B'). (D) A histogram of the mesh sizes from multiple relaxed medioapical arrays demonstrates that the mean size is 473 ± 210 nm; n=5 cells from 3 embryos including data shown in Figure 3.